

## Lysine-60 in Copper Chaperone Atox1 Plays an Essential Role in Adduct Formation with a Target Wilson Disease Domain

Faiza Hussain,<sup>†</sup> Agustina Rodriguez-Granillo,<sup>†</sup> and Pernilla Wittung-Stafshede<sup>\*,‡</sup>

Department of Biochemistry and Cell Biology, Rice University, 6100 Main Street, Houston, Texas 77251, and Department of Chemistry, Chemical Biological Center, Umeå University, 901 87 Umeå, Sweden

Received July 14, 2009; E-mail: Pernilla.wittung@chem.umu.se

Using near-UV circular dichroism as a new tool to probe Atox1–Wilson disease protein (WD) metal-binding domain interactions, in combination with molecular dynamics (MD) simulations, we here demonstrate that Atox1 forms a stable Cu-dependent adduct with a metal-binding domain of WD which is modulated by key residues in proximity to the metal-binding site.

Cu homeostasis is regulated by molecular mechanisms in which the metal is sequestered by carrier proteins. Human Atox1 is a prototype of the structurally conserved prokaryotic and eukaryotic soluble metallochaperones and target metal-binding domains (MBDs) of the P<sub>1B</sub>-type ATPases. These proteins possess a ferredoxin-like fold and bind Cu(I) via Cys<sub>2</sub> coordination in a MxCxxC motif<sup>1</sup> (Figure 1). Atox1 delivers Cu to the MBDs of the human P<sub>1B</sub>-type ATPases, Menkes (ATP7A), and Wilson (ATP7B or WD) disease proteins that are localized in the Golgi membrane, via direct protein–protein interactions. Cu is subsequently translocated from the cytoplasm to the Golgi lumen for incorporation into cuproenzymes.

M10 in the MxCxxC motif is not involved in metal ligation<sup>1,2</sup> but acts as a tether to modulate Cu-binding loop structure.<sup>3,4</sup> Adjacent to M10 in the sequence is always a polar residue; in eukaryotes, T11 in this position is proposed to hydrogen bond with the first Cys of the target MBD during Cu transfer<sup>5</sup> (Figure 1). Sequentially distant but structurally proximal to the metal binding site is residue 60 which is an invariant Lys in eukaryotic Cu chaperones but Tyr in prokaryotes.<sup>1</sup> Cu-dependent interactions between Atox1 and target domains have been characterized by several methods, including yeast two-hybrid analysis and NMR titrations.<sup>6–9</sup> Although Atox1 delivers Cu to all six WD MBDs *in vitro*, it forms detectable heterocomplexes with only a subset (i.e., WD1, WD2, and WD4).<sup>9</sup> Here, we probed the role of conserved residues near the Cu-binding site of Atox1 (by preparing M10A, T11A, K60A, and K60Y variants) to decipher their role in Atox1-mediated Cu transfer to a WD MBD. All variants were folded and exhibited high thermal stability (Supporting Information).

Since preferential interaction of Atox1 with WD4 has been postulated by both experiments<sup>7,8</sup> and simulations,<sup>10</sup> we assessed Atox1-mediated Cu delivery to WD4 using spectral changes in the near-UV circular dichroism (CD) region (pH 7.5, 20 °C). The near-UV CD region (250–320 nm) is dominated by ligand-to-metal charge transfer from Cys-S to Cu (and minor contributions from aromatic residues). Cu additions to all Atox1 variants and WD4 result in distinct near-UV CD changes in accord with Cu binding (Figure S1). Metal binding is also supported by higher thermal stability of Cu-loaded forms as compared to the apo-forms (Table S1).

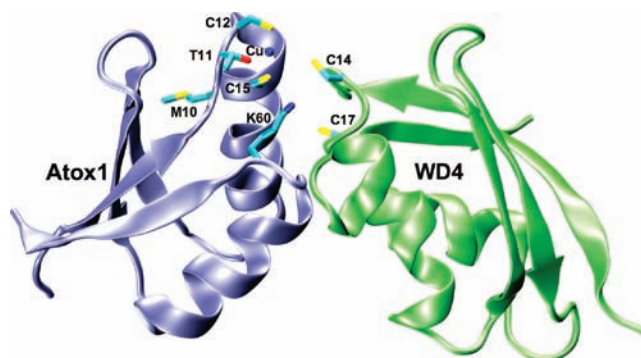


**Figure 1.** Structure of heterocomplex between Cu-Atox1 (blue) and apo-WD4 (green) (see Supporting Information for details of adduct generation). Key residues in Atox1 (i.e., M10, T11, C12, C15, and K60) as well as C14 and C17 in WD4 are highlighted in sticks.

Combination of CD spectra for apo- and holo-forms was used to generate theoretical signals for 0 and 100% transfer of Cu from Atox1 to WD4. However, upon mixing Cu-loaded wild-type (WT) Atox1 with apo-WD4, a distinct spectrum with a positive (295 nm) and negative (265 nm) peak (Figure 2A) was observed. This suggests heterocomplex formation with a unique Cu site containing 3 or 4 Cys ligands instead of 2. The Atox1–WD4 heterocomplex was isolated by gel filtration, and the presence of Cu was demonstrated by ICP-MS (Figure 2B). Also, the elution peak for WD4 contained Cu in agreement with a mixture of Cu-containing heterocomplex and Cu transfer to WD4. Mixing only apo-proteins did not result in complex formation, but adding Cu to a preincubated mixture of the apo-proteins or mixing Cu–WD4 and apo-Atox1 (reverse Cu transfer) induced complex formation based on near-UV CD (Figure S2A). Previous NMR data have suggested the formation of Cu-dependent heterocomplexes that are in fast exchange with the individual proteins after addition of apo-WD4 to Cu-Atox1.<sup>7</sup> Self-dimerization of individual holo-proteins was ruled out by gel filtration experiments (Figure S2B).

Heterocomplex formation between Cu-loaded Atox1 mutants and apo-WD4 was also investigated by near-UV CD and gel filtration combined with Cu quantification (Figure 2AB). T11A and M10A Atox1 variants formed stable adducts with WD4 with similar amounts of Cu in the heterocomplex peak as WT Atox1–WD4 complex; there was less Cu in the monomeric WD4 peak in the case of T11A Atox1. No heterocomplex was detected upon mixing Atox1 K60 variants and WD4, and less Cu was found in the WD4 peak (Figure 2B). Thus, the absence of K60 weakens the heterocomplex and also diminishes the transfer of Cu to WD4. The CD data on the mutant mixtures (Figure 2A) qualitatively agree with the gel filtration results: the unique CD spectrum implying a heterocomplex is also observed for M10A and T11A Atox1 mutants

<sup>†</sup> Rice University.  
<sup>‡</sup> Umeå University.

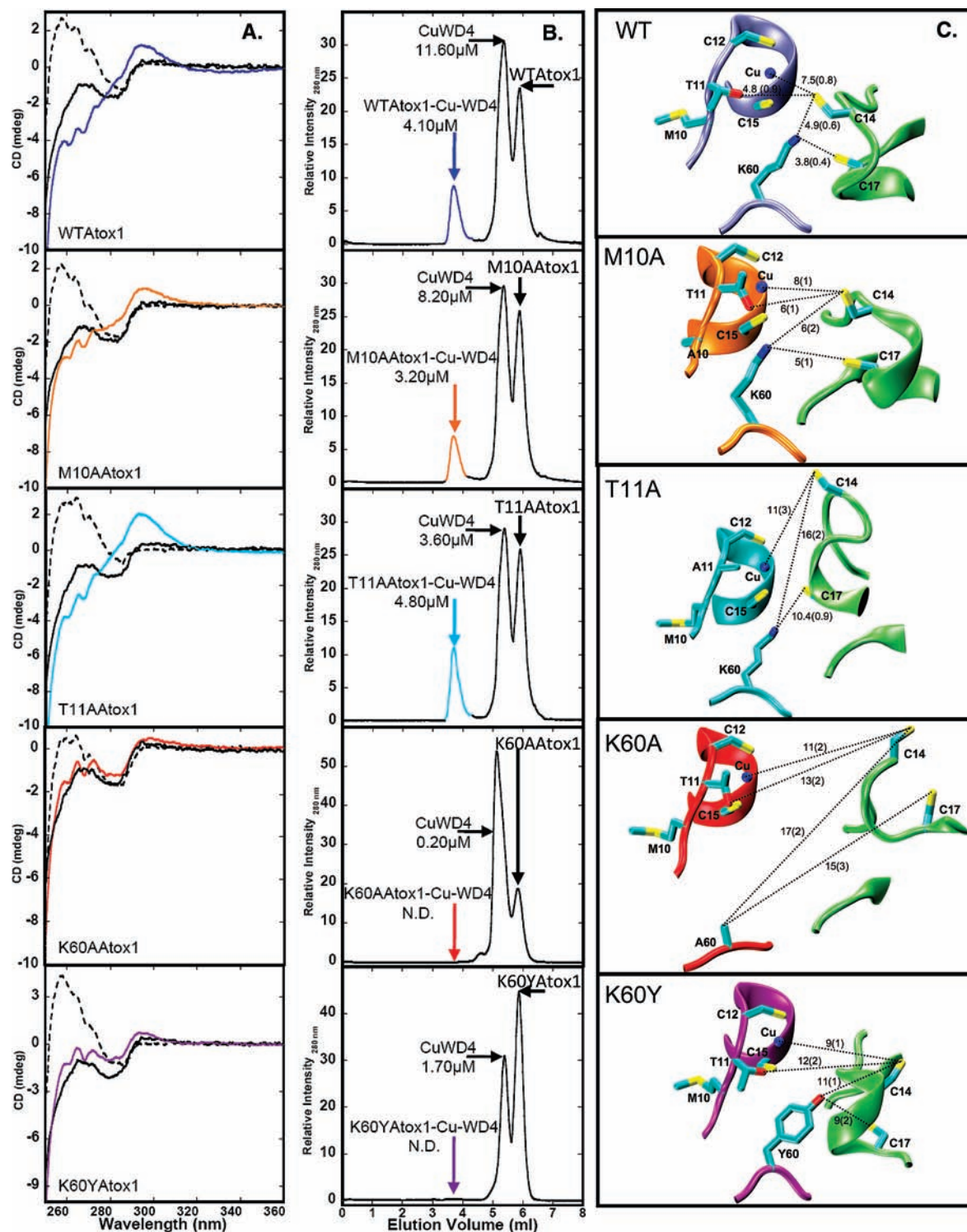


**Figure 2.** (A) Near-UV CD of Cu-Atox1 variants (initial  $100 \mu\text{M}$ ) mixed with apo-WD4 (initial  $100 \mu\text{M}$ ) in 1:1 ratio; expected curves for 0 (dashed line) and 100% (black solid line) Cu transfer based on combinations of CD spectra for individual apo/holo proteins are also shown. (B) Gel filtration traces for each mixture ( $500 \mu\text{M}$  Cu-Atox1 mixed with  $500 \mu\text{M}$  apo-WD4 in 1:1 ratio prior to injection) with the different species (based on SDS PAGE) and amount of Cu indicated (quantified by ICP-MS). N.D., not detected. (C) Zoom-in of Cu-Atox1 and apo-WD4 active sites (Cu and  $\alpha 2$ - $\beta 4$  loops) in each heterocomplex; the final structure (except for K60A) of each MD simulation is shown. Distances between atoms (in Å) correspond to the average and standard deviation values during the last 10 ns. For K60A, the structure corresponds to the snapshot from  $\sim 20$  ns, before the proteins interact nonspecifically, and the distances correspond to the last 10 ns of those  $\sim 20$  ns.

mixed with WD4, whereas, for the K60 mutant mixtures, these CD spectral features are less pronounced. We note that there is still some character of the heterocomplex spectrum in the CD traces for the K60 mutant samples. Since higher protein concentrations are present in the CD experiments as those in the eluted gel filtration

peaks, a small fraction of heterocomplex may form at the CD conditions that does not survive gel filtration. The CD spectra are linear combinations of signals for many species (apo- and holo-forms of Atox1 and WD4, heterocomplex) present at different levels; thus, the CD data are only qualitative.

**Table 1.** Free Energy ( $\Delta G$ ) of Cu-Atox1-WD4 Heterocomplex Formation for Atox1 Variants (WT<sup>10</sup>), Including Its Different Energetic Contributions: Intermolecular Van Der Waals Interactions (vdW), Change in Nonpolar Solvation Energy (cavity), Intermolecular Coulomb Interactions (electrostatic) and Change in Reaction Field Energy (field)<sup>a</sup>

	$\Delta G$	vdW	cavity	electrostatic	field
WT	$-9.5 \pm 0.4$	$-50 \pm 4$	$-9.7 \pm 0.4$	$-172 \pm 12$	$169 \pm 10$
M10A	$-9.4 \pm 0.7$	$-51 \pm 6$	$-9.3 \pm 0.6$	$-136 \pm 14$	$134 \pm 12$
T11A	$-9.7 \pm 0.5$	$-57 \pm 5$	$-9.7 \pm 0.6$	$-119 \pm 15$	$121 \pm 13$
K60A	$-6.1 \pm 0.8$	$-28 \pm 6$	$-5.0 \pm 1.0$	$-65 \pm 18$	$68 \pm 16$
K60Y	$-7.9 \pm 0.5$	$-43 \pm 4$	$-8.4 \pm 0.6$	$-95 \pm 18$	$98 \pm 15$

<sup>a</sup>All energy values are in kcal/mol; errors correspond to standard deviation. Reported energy values correspond to average of 100 calculations based on the last 10 ns of MD simulations. For K60A, the analysis was done for the last 10 ns from the first  $\sim 20$  ns, before the proteins interact nonspecifically.

We previously showed that the K60A<sup>3</sup> and K60Y (FH, PWS, unpublished) mutations enhance both the rate and extent of Atox1 dissociation from an Atox1-Cu-BCA intermediate formed during chelator-mediated dissociation of Cu from Atox1.

To explore the roles of M10, T11, and K60 in Cu-Atox1-WD4 adduct stability, we performed MD simulations of the different heterocomplexes (Supporting Information) and compared the results to our WT heterocomplex data.<sup>10</sup> In agreement with the *in vitro* data, all heterocomplexes are stable during each MD simulation of more than 50 ns, except that involving the K60A mutant (Figure S3) which is only stable for the first  $\sim 20$  ns, followed by a conformational change in which the proteins interact nonspecifically. Instability of the K60A(Atox1)-WD4 complex is also evidenced by a  $>2$ -fold increase in fluctuations with respect to WT(Atox1)-WD4 (Figure S4).

In the WT(Atox1)-WD4 heterocomplex,<sup>10</sup> a stable interaction network keeps the two Cu-binding sites in close contact (Figure 2C). This intermolecular network is disrupted in the mutants, causing WD4's Cys to be more distant from holo-Atox1's Cu site (Figure 2C). In M10A and T11A Atox1 complexes, WD4's Cys always face the Atox1 surface, whereas, in the K60 Atox1 mutants, these Cys primarily face the opposite side, which explains the lower extent of Cu transfer to WD4 found experimentally. M10A(Atox1)-WD4 shows behavior closest to that of WT(Atox1)-WD4, consistent with the distance of this residue from the interacting surface. Lack of a polar residue in position 11 of Atox1, as in T11A, disrupts hydrogen bond interactions with WD4's active site. Thus, WD4's active site moves further away, although the two proteins remain in a tight and compact complex. This observation corroborates with the higher proportion of T11A(Atox1)-WD4 adduct but decreased amount of Cu transfer to WD4 detected (Figure 2B). In the K60 substitutions, the proteins lose both intermolecular side chain and backbone interactions. However, during at least 50 ns of the simulation, replacement of K60 by a hydrogen bond donor (Tyr) prevents rupture of the heterocomplex, as opposed to the impact of an Ala substitution.

To quantify the strength of interprotein interactions, we estimated the free energy of heterocomplex formation (Table 1). Whereas M10A and T11A mutations do not alter overall heterocomplex stability, K60A and K60Y Atox1 mutations have detrimental effects on adduct stability, in concordance with the absence of detectable complexes in experiments. The intermolecular Coulombic interac-

tion is greatly reduced in the K60 mutant complexes (Table 1). Moreover, the nonpolar solvation energy is reduced only in the K60 mutants, evidencing a reduction in the packing of the complex. Thus, the interacting surface between Atox1 and WD4 appears to be the result of the sum of small interactions, in which K60 plays a dominant role. This interface can be disrupted with at least one substitution at position 60 in Atox1, which points to the subtle balance of forces that contribute to heterocomplex stability, as also recently suggested for a similar Atox1-MBD adduct based on NMR data.<sup>11</sup>

We conclude that near-UV CD is a useful tool to investigate this family of proteins without tags (that may cause artifacts) that can provide insights complementary to NMR and computations. We discovered that mixing Cu-Atox1 (WT, M10A, and T11A) with the apo-form of a target WD domain (WD4) yields a mixture of stable Cu-containing heterocomplexes and WD4. Atox1 interacts with WD4 via a weak interface that can be disrupted by a single mutation in Atox1. Mutation of K60 in Atox1 weakens heterocomplex formation and Cu transfer to WD4; the heterocomplex is thus an intermediate on the transfer path. Chaperone-target electrostatic complementarity (provided by K60) facilitates heterocomplex stability and Cu transfer from Atox1 to WD4. With increasing reports of Cu involvement in human diseases,<sup>12</sup> a mechanistic understanding and new experimental approaches for detecting protein-mediated Cu transport are vital.

**Acknowledgment.** We thank K. S. Matthews, J. S. Olson, and A. Crespo for helpful discussions and D. Huffman for WD4 plasmid. This work was supported by the Shared University Grid at Rice (NSF EIA-0216467), partnership between Rice University, Sun Microsystems, and Sigma Solutions, Inc. P.W.S. acknowledges support from the Swedish Science Research Council, Kempe, and Wallenberg foundations.

**Supporting Information Available:** Experimental and computational methods. Figures S1 to S4, Table S1. This material is available free of charge via the Internet at <http://pubs.acs.org>.

## References

- (1) Arnesano, F.; Banci, L.; Bertini, I.; Ciofi-Baffoni, S.; Molteni, E.; Huffman, D. L.; O'Halloran, T. V. *Genome Res.* **2002**, *12*, 255–71.
- (2) Anastassopoulou, I.; Banci, L.; Bertini, I.; Cantini, F.; Katsari, E.; Rosato, A. *Biochemistry* **2004**, *43*, 13046–53.
- (3) Hussain, F.; Olson, J. S.; Wittung-Stafshede, P. *Proc. Natl. Acad. Sci. U.S.A.* **2008**, *105*, 11158–63.
- (4) Rodriguez-Granillo, A.; Wittung-Stafshede, P. *Biochemistry* **2009**, *48*, 960–72.
- (5) Wernimont, A. K.; Huffman, D. L.; Lamb, A. L.; O'Halloran, T. V.; Rosenzweig, A. C. *Nat. Struct. Biol.* **2000**, *7*, 766–71.
- (6) Larin, D.; Mekios, C.; Das, K.; Ross, B.; Yang, A. S.; Gilliam, T. C. *J. Biol. Chem.* **1999**, *274*, 28497–504.
- (7) Achila, D.; Banci, L.; Bertini, I.; Bunce, J.; Ciofi-Baffoni, S.; Huffman, D. L. *Proc. Natl. Acad. Sci. U.S.A.* **2006**, *103*, 5729–34.
- (8) Banci, L.; Bertini, I.; Cantini, F.; Rosenzweig, A. C.; Yatsunyk, L. A. *Biochemistry* **2008**, *47*, 7423–9.
- (9) Banci, L.; Bertini, I.; Cantini, F.; Massagni, C.; Migliardi, M.; Rosato, A. *J. Biol. Chem.* **2009**, *284*, 9354–60.
- (10) Rodriguez-Granillo, A.; Crespo, A.; Wittung-Stafshede, P. *Biochemistry* **2009**, *48*, 5849–63.
- (11) Banci, L.; Bertini, I.; Calderone, V.; Della-Malva, N.; Felli, I. C.; Neri, S.; Pavelkova, A.; Rosato, A. *Biochem. J.* **2009**, *422*, 37–42.
- (12) Crouch, P. J.; Hung, L. W.; Adlard, P. A.; Cortes, M.; Lal, V.; Filiz, G.; Perez, K. A.; Nurjono, M.; Caragounis, A.; Du, T.; Laughton, K.; Volitakis, I.; Bush, A. I.; Li, Q. X.; Masters, C. L.; Cappai, R.; Cherny, R. A.; Donnelly, P. S.; White, A. R.; Barnham, K. J. *Proc. Natl. Acad. Sci. U.S.A.* **2009**, *106*, 381–6.

JA9058266